Planta (2007) 225:919–933
DOI 10.1007/s00425-006-0411-0

ORIGINAL ARTICLE

Accumulation of multiple-repeat starch-binding domains (SBD2–SBD5) does not reduce amylose content of potato starch granules

Farhad Nazarian Firouzabadi · Jean-Paul Vincken · Qin Ji · Luc C. J. M. Suurs · Alain Buléon · Richard G. F. Visser

Received: 24 July 2006 / Accepted: 14 September 2006 / Published online: 13 October 2006

Abstract This study investigates whether it is possible to produce an amylose-free potato starch by displacing the amylose enzyme, granule-bound starch synthase I (GBSSI), from the starch granule by engineered, high-affinity, multiple-repeat family 20 starch-binding domains (SBD2, SBD3, SBD4, and SBD5). The constructs were introduced in the amylose-containing potato cultivar (cv. Kardal), and the starches of the resulting transformants were compared with those of SBD2-expressing amylose-free (*amf*) potato clones. It is shown that a correctly sized protein accumulated in the starch granules of the various transformants. The amount of SBD accumulated in starch increased progressively from SBD to SBD3; however, it seemed as if less SBD4 and SBD5 was accumulated. A reduction in amylose content was not achieved in any of the transformants. However, it is shown that SBDn expression can affect physical processes underlying granule assembly, in both genetic potato backgrounds, without altering the primary structure of the constituent starch polymers and the granule melting temperature. Granule size distribution of the starches obtained from transgenic Kardal plants were similar to those from untransformed controls, irrespective of the amount of SBDn accumulated. In the *amf* background, granule size is severely affected. In both the Kardal and *amf* background, apparently normal oval-shaped starch granules were composed of multiple smaller ones, as evidenced from the many "Maltese crosses" within these granules. The results are discussed in terms of different binding modes of SBD.

Keywords Amylose · Granule-bound starch synthase · Starch-binding domain · Starch biosynthesis · Transgenic potato plant

Abbreviations

SBD	Starch-binding domain
SBD2	Double starch-binding domain
GBSSI	Granule-bound starch synthase I
amf	Amylose-free
LM	Light microscopy
SEM	Scanning electron microscopy
DSC	Differential scanning calorimetry
KD-UT	Kardal untransformed
amf-UT	Amylose-free mutant untransformed
KDS	Kardal transformant containing SBD gene

F. N. Firouzabadi · J.-P. Vincken · Q. Ji · L. C. J. M. Suurs · R. G. F. Visser (✉)
Graduate School Experimental Plant Sciences, Laboratory of Plant Breeding, Wageningen University, P.O. Box 386, 6700 AJ Wageningen, The Netherlands
e-mail: richard.visser@wur.nl

F. N. Firouzabadi
Agronomy and plant breeding group, Faculty of Agriculture, University of Lorestan, P.O. Box 465, Khorramabad, Iran

J.-P. Vincken
Laboratory of Food Chemistry, Wageningen University, P.O. Box 8129, 6700 EV Wageningen, The Netherlands

Q. Ji
Department of Biology, HuaiYin Teachers College, 223300 Huaian, China

A. Buléon
Laboratoire de Physico-chimie des Macromolécules, Institut National de la Recherche Agronomique, BP 71627, 44316 Nantes Cedex 3, France

KDSS Kardal transformant containing double SBD gene
KDS3 Kardal transformant containing triple SBD gene
KDS4 Kardal transformant containing quadruple SBD gene
KDS5 Kardal transformant containing pentuple SBD gene
*amf*S *amf* mutant transformed with SBD gene
*amf*SS *amf* mutant transformed with double SBD gene

Introduction

Potato starch granules are composed of two polysaccharides, the more or less unbranched amylose (approximately 20%) and the highly branched amylopectin (approximately 80%) (Kossmann and Lloyd 2000). From an industrial viewpoint, the presence or absence of amylose is important, because it greatly determines the suitability of starch for different applications (Visser et al. 1997a, b). Properties as retrogradation of starch pastes (Visser et al. 1997b), poor transparency of starch gels and low adhesiveness (Visser et al. 1997a), poor freeze-thaw stability (Jobling et al. 2002), and high granule melting temperatures (Schwall et al. 2000) are all correlated with a high (apparent) amylose content of potato starch. Therefore, the *in planta* modulation of the amount of amylose of potato starch granules has been an important objective for the starch industry.

Various transgenic approaches have been explored for modifying the amylose content of potato starch. Granules with a very high apparent amylose content (~70%) were obtained by the simultaneous antisense inhibition of both potato starch-branching enzyme isoforms (Schwall et al. 2000). An essentially amylose-free starch could be obtained by down-regulation of the activity of granule-bound starch synthase I (GBSSI), the amylose enzyme (Kuipers et al. 1994), demonstrating that GBSSI is the only synthase involved in amylose synthesis. Interestingly, the amount of amylose of potato starch granules could also be reduced (to ~13%) by decreasing the ADP-glucose pool size (antisense AGPase; Lloyd et al. 1999b). The fact that GBSSI has a lower affinity (higher Km) for ADP-glucose in comparison with (at least some) other starch synthases may explain this observation (Edwards et al. 1999a). Thus, it seems as if GBSSI is the first synthase to suffer from a low ADP-Glc concentration, leading to the production of less amylose.

In a previous paper we have shown that microbial starch-binding domains (SBDs) can be accumulated in starch granules during the starch biosynthesis process, without affecting the amount of amylose (Ji et al. 2003; Kok-Jacon et al. 2003). It was also shown that more SBD could be incorporated in the granules of the amylose-free (*amf*) potato mutant. One explanation for that observation could be that GBSSI and SBD bind similar sites in the granule, and that GBSSI has the highest affinity for starch of the two proteins. Therefore, we engineered a high-affinity starch-binding domain by fusing two similar SBDs via a Pro-Thr rich linker peptide (SBD2). It was shown that SBD2 had an approximately ten fold higher affinity for starch, and that much higher amounts of this protein could be accumulated in *amf* starch granules than of SBD (Ji et al. 2004). Moreover, expression of SBD2 in the *amf* potato background resulted in an approximately two-fold reduction of the starch granule size. In contrast, others have shown that expression of a tandem SBD in *Arabidopsis* increased starch granule size, particularly in the *sex 1–1* mutant, which has a mutation in the R1 gene involved in the phosphorylation of starch (Howitt et al. 2006). In this study we investigated whether it is possible to obtain an amylose-free starch by introducing SBD2 in a wild type potato background. Additionally, we have engineered a SBD3, SBD4, and SBD5, consisting of three, four, and five SBD repeats, respectively, separated by Pro-Thr rich linkers. Our hypothesis was that multiple appended SBDs might be strong enough to displace GBSSI from the starch granule.

Materials and methods

Constructs for transformation

The pBIN19/SBD2 plasmid was used for the expression of SBD2 protein in potato plants; for the preparation of this construct we refer to Ji et al. (2004). The gene was expressed in potato plants under the control of the tuber-specific potato GBSSI promoter. Amyloplast entry of SBD2 was mediated by the potato GBSSI transit peptide. The construct for expression of SBD3 (pBIN19/SBD3) in potato plants was made as follows. The pBIN19/SBD3 construct was assembled from the pUC19/SBD2 (Ji et al. 2004). A SBD-encoding sequence was amplified by polymerase chain reaction proof-reading *Pfu* turbo DNA polymerase (Stratagene, Cambridge, UK) with the primers 5′-ATAGCAAC**CTCGAG**TAGTACCATGGCCGGG-GATCAG-3′ and 5′-CGCCTGGTGTTCTAGAATT CG**GTCGAC**GGGGT-3′, which contained an *Xho*I

and *Sal*I at their 5′-ends, respectively. The pUC19/SBD (Ji et al. 2003) plasmid was used as a template. The amplified fragment was inserted into pUC19/SBD2, which was opened with *Sal*I, to give the pUC19/SBD3 plasmid (*Xho*I and *Sal*I have compatible overhangs). The orientation of the inserted fragment was checked by digestion with *Bgl*II. The gene sequence contains two *Bgl*II sites, one at the beginning of the first linker, and one at the beginning of the second linker. The length of the *Bgl*II–*Bgl*II fragment in the correct orientation should be 387 nucleotides. In order to verify its correctness, the construct was sequenced (long runs). In a similar way, the pUC19/SBD4 plasmid was obtained. Briefly, the *Xho*I–*Sal*I fragment (see above) was cloned in pUC19/SBD3, after opening this plasmid with *Sal*I. The orientation of the insert was checked by digestion with *Hin*dIII, and by sequencing. Similar procedures were followed for generating pUC19/SBD5. After digestion of the plasmids pUC19/SBD3, pUC19/SBD4, and pUC19/SBD5 with *Hpa*I and *Kpn*I, the *Hpa*I–*Kpn*I fragment was inserted into the corresponding sites of the pBIN19/SBD2 to generate the pBIN19/SBD3, pBIN19/SBD4, and pBIN19/SBD5, respectively. The predicted molecular masses of the SBD3, SBD4, and SBD5 produced in plants is 39,315, 53,157, and 66,999 Da, respectively, excluding the transit peptide.

Plant transformation and regeneration

The pBIN19/SBD2, pBIN19/SBD3, pBIN19/SBD4, and pBIN19/SBD5 plasmids were introduced into the amylose-containing potato (*Solanum tuberosum*) cultivar (cv. Kardal; Laboratory of Plant Breeding, Wageningen University, P.O. Box 386, 6700 AJ Wageningen, The Netherlands) via *Agrobacterium*-mediated transformation described by Visser (1991). More than 50 independent shoots were harvested for each genotype. Shoots were tested for root growth on a kanamycin-containing (100 mg/l) MS30 medium (Murashige and Skoog 1962). For each genotype, 50 transgenic, root-forming, shoots were multiplied and 5 plants of each transgenic clone were transferred to the greenhouse for tuber development. In addition, ten untransformed controls were grown in the greenhouse.

Determination of SBDn transcript levels

Total RNA extraction was performed according to Kuipers et al. (1994). Total RNA was extracted from 5 g (fresh weight) of potato tuber material. The amount of RNA was determined spectrophotometrically in each sample. The RNA concentration was verified by running an appropriate volume corresponding to 40 μg on a 0.8% w/w agarose gel. Based on a spectrophotometric RNA determination, similar amounts of total RNA were fractionated on a 1.5% (w/v) agarose-formaldehyde gel, and transferred to a Hybond N nylon membrane (Amersham, Little Chalfont, UK). The membrane was hybridized with a [^{32}P]-labeled *Nco*I–*Bam*HI DNA fragment of SBD2 as a probe; labelling was performed using a *redi*prime^{TM}II kit (Amersham) according to the instructions of the manufacturer.

Isolation of tuber starch

All tubers derived from the five plants of each greenhouse-grown clone were combined, and their peels were removed in an IMC VC7T Peeler (Spangenberg, Waardenburg, The Netherlands). The peeled tubers were homogenized in a Sanamat Rotor (Spangenberg), and filtered through a sieve to remove particulate material. The resulting homogenate was allowed to settle in 0.01% (w/w) $N_2S_2O_5$ for 20 min at 4°C, and the tuber juice was collected for later use, and stored at −20°C. The starch sediment was washed three times with water, and finally air-dried at room temperature (Ji et al. 2004).

Determination of SBD content of starches by Western dot blot analysis

A 12.5% sodium dodecyl sulfate-polyacrylamide gel (50 mm × 50 mm × 3 mm) with nine, equally-spaced, holes (Ø = 9 mm) was placed in contact with a similarly-sized Hybond ECL nitrocellulose membrane (Amersham). For determining the SBD2, SBD3, SBD4, and SBD5 content, 20 mg of (transgenic) starch was boiled for 5 min with 200 μL of 2× SDS sample buffer (Laemmli 1970). After cooling to room temperature, the starch gel was transferred into one of the holes. The proteins in the transgenic starch gels were blotted to the membrane using a PhastSystem (Pharmacia, Uppsala, Sweden; 20 V, 25 mA, 15°C, 45 min) (Ji et al. 2003). The protein was identified with anti-SBD antibody according to the method described by Ji et al. (2003).

Determination of the expression of major starch biosynthetic genes

Gene expression of major starch biosynthetic enzymes was measured using quantitative real time PCR (qRT-PCR) analysis. The PCR reaction consisted of 25 μl of a mixture containing: 1× PCR buffer, 1.5 mM $MgCl_2$, 0.2 mM dNTPs, 0.2 μM of each sequence-specific

primers 3 µl SYBR Green I (1:15,000 diluted), 3 µl of transcribed cDNA, and 0.5 U of Taq polymerase. Specific primers for starch branching enzyme I (SBEI), sucrose synthase (Susy), ADP-glucose pyrophosphorylase (AGPase), starch synthase III (SSSIII) (according to Kok-Jacon et al. 2005), for three isoamylase isoforms (Stisa1, Stisa2 and Stisa3; Bustos et al. 2004), and for the internal control gene ubiquitin (ubi3; 5′-TTCC GACACCATCGACAATGT-3′ and 5′-CGACCAT CCTCAAGCTGCTT-3′) were designed by the primer express software (version 1.5, PE Applied Biosystems, CA, USA). In qRT-PCR analysis, quantification is based on C_t values. The C_t (cycle threshold) is a measurement taken during the exponential phase of amplification when limiting reagents and small differences in starting amount have not yet influenced the PCR efficiency. C_t is defined as the cycle at which fluorescence is first detectable above background, and is inversely proportional to the log of the initial copy number. Each reaction was performed in triplicate and the corresponding C_t values were determined. The C_t values of each qRT-PCR reaction were normalized in relation to the C_t value corresponding to the Ubi3 gene. These values were then used to determine the changes in gene expression among the different transformants and their corresponding control plants.

Electrophoretic separation of granule proteins SBDn and GBSSI

Fifty milligram of starch was boiled for 2 min in 1 ml of SDS sample buffer, containing 5% (v/v) β-mercaptoethanol. The gelatinized samples were centrifuged for 10 min at 14,000*g*. Twenty-five microliter of supernatant were loaded onto a 12% polyacrylamide gel (145 mm × 95 mm × 3 mm), and the proteins were separated by electrophoresis. Subsequently, the proteins were transferred onto a Hybond ECL membrane (Amersham), and detected using anti-SBD as described in the previous section, or anti-GBSSI polyclonal antibody (Vos-Scheperkeuter et al. 1986) in a 1:250 dilution.

Determination of SBDn content of potato juice

SBD2, SBD3, SBD4 and SBD5 proteins in the soluble fraction of potato tubers were determined as follows. Five hundred microliter of tuber juice was freeze-dried. The dried material was dissolved in 200 µl of SDS sample buffer, containing 5% (v/v) β-mercaptoethanol. In order to make the sample suitable for Western dot blot procedure, the mixture was boiled for 5 min in the presence of 20 mg starch from the control samples. The resulting starch gel was applied to one of the holes in the sodium dodecyl sulfate-polyacrylamide gel. The rest of the procedure was conducted in the same way as described for granule-bound SBD2 (Ji et al. 2004).

Analysis of physico-chemical properties of starch granules

The average granule size and granule size distribution of the (transgenic) starches were determined in triplicate with a Coulter Multisizer II, equipped with an orifice tube of 200 µm (Beckman-Coulter, High Wycombe, UK). Approximately 10 mg of starch was dispersed in 160 ml of Isoton II. The granule size distributions were recorded by counting approximately 50,500 (±500) particles. The coincidence (the frequency of two granules entering the tube at the same time, and consequently being counted as one) was set at 10%.

Starch granule morphology and birefringence were investigated by light microscopy (LM, Axiophot, Oberkochen, Germany). Starch granules were stained with a 20× diluted Lugol solution (1% I_2/KI). For determining the birefringence of the granules the polarized light device was used. For scanning electron microscopy (SEM, JEOL 6300F, Japanese Electron Optics Laboratory, Tokyo, Japan), dried starch samples spread on silver tape and mounted on a brass disc were coated with a 20 nm platinum layer. Samples were then examined with a scanning electron microscope operating at an accelerating voltage of 1.5–3.5 keV. The working distance was 9 mm.

The apparent amylose content was determined according to the method described by Hovenkamp-Hermelink et al. (1988).

The temperature at which starch granules start to gelatinize was determined by differential scanning calorimetry (DSC) using a Perkin–Elmer Pyris 1 (Perkin–Elmer, Vlaardingen, The Netherlands), equipped with a Neslab RTE-140 glyco-cooler (Ji et al. 2003).

Prior to X-ray diffraction, the water content of the starch was equilibrated at 90% of relative humidity (RH) under partial vacuum in presence of a saturated barium chloride solution. The samples (20 mg) were then sealed between two tape foils to prevent any significant change in water content during the measurement. Diffraction diagrams were recorded using an INEL spectrometer (Artenay, France) working at 40 kV and 30 mA, operating in the Debye-Scherrer transmission mode. The X-ray radiation $CuK\alpha_1$ ($\lambda = 0.15405$ nm) was selected with a quartz monochromator. Diffraction diagrams were recorded during 2 h exposure periods, with a curve position sensitive detector

(INEL CPS 120). Relative crystallinity was determined after normalization of all recorded diagrams at the same integrated scattering between 3 and 30° (2θ). B-type recrystallized amylose was used as crystalline standard, after scaled subtraction of an experimental amorphous curve in order to get nul intensity in the regions without diffraction peaks. Dry extruded potato starch was used as the amorphous standard. The degree of crystallinity of samples having a pure polymorphic type was determined using the method initially developed for cellulose (Wakelin et al. 1959). The percentage of crystallinity was taken as the slope of the line $(I_{sample}-I_{amor})_{2\theta}=f(I_{crys}-I_{amor})_{2\theta}$ where I_{sample}, I_{amor} and I_{crys} are the diffracted intensity of the sample, the amorphous and the crystalline standards, respectively.

Determination of chain-length distribution

For chromatography, 5 mg of (transgenic) starch was suspended in 250 µl of DMSO, and the starch was gelatinized by keeping this suspension for 15 min in a boiling water bath. Subsequently, the solution was cooled down to 40°C, and 700 µl of 50 mM NaOAc buffer (pH 4.0), containing sufficient isoamylase (Hayashibara Biochemical, Okayama, Japan) to debranch the starch polymers completely, was added. After 2 h of incubation at 40°C, the enzyme was inactivated in a boiling water bath for 10 min. To each sample, 1 ml of 25% DMSO was added, and the samples were centrifuged (7,500*g*, 2 min). For HPAEC, the supernatant was diluted five times with a 25% DMSO solution; for HPSEC, the samples were used as such.

HPSEC was performed on a P680 HPLC pump system (Dionex, Sunnyvale, CA, USA) equipped with three TSKgel SWXL columns in series (a G3000 and two G2000; 300× 7.5 mm; Montgomeryville, USA) in combination with a TSKgel SWXL guard column (40× 6 mm) at 35°C. Aliquots of 100 µl were injected using a Dionex ASI-100 Automated Sample Injector, and subsequently eluted with 10 mM NaOAc buffer (pH 5.0) at a flow rate of 0.35 mlmin (3 h run). The effluent was monitored using a RID-6A refractometer (Shimadzu, Kyoto, Japan). The system was calibrated using dextran standards (10, 40, 70, 500 kDa; Pharmacia). Dionex Chromeleon software version 6.50 SP4 Build 1000 was used for controlling the HPLC system and data processing.

HPAEC was performed on a GP40 gradient pump system (Dionex) equipped with a CarboPac PA 100 column (4 × 250 mm^2; Dionex) at 35°C. The flow rate was 1.0 ml/min and 20 µl sample was injected with a Dionex AS3500 automated sampler. Two eluents were used, eluent A (100 mM NaOH) and eluent B (1 M NaOAc in 100 mM NaOH), for mixing the following gradient: 0→5 min, 100% eluent B (rinsing phase); 5→20 min, 100% eluent A (conditioning phase); 20→25 min, linear gradient from 0→20% eluent B (100→80% eluent A); 25→50 min, linear gradient from 20→35% eluent B (80→65% eluent A); 50→55 min, linear gradient from 35→50% eluent B (65→50% eluent A); 55→60 min, 50% eluent B (50% eluent A). The sample was injected at 20 min. The eluent was monitored by an ED40 electrochemical detector in the pulsed amperometric mode (Dionex).

Determination of starch content

Approximately 50 mg of potato tuber material was dissolved in 0.5 ml of 25% HCl and 2 ml of dimethylsulfoxid (DMSO) for 1 h at 60°C. After incubation, the mixture was neutralized with 5 M NaOH and diluted in 0.1 M citrate buffer (pH 4.6) to a final volume of 10 ml. Twenty microliter of the hydrolyzed starch sample was determined enzymatically using a test kit (Boehringer, Mannheim, Germany), according to the instructions of the manufacturer. The values are an average of three independent measurements.

α-Amylase treatment of starch granule preparations

Twenty milligrams of *amf*SS#3 or KDSS#7, as well as their respective control starches, was suspended in 1 ml of 50 mM phosphate buffer (pH 6.9), and treated with 5 U of porcine pancreas α-amylase (Sigma-Aldrich Chemie B.V., Zwijndrecht, The Netherlands) for 4 h at 25°C. Samples without α-amylase addition served as controls. After incubation, the samples were centrifuged (7,500*g*, 10 min). The starch pellets were washed three times with water, and air-dried. The dried starch granules were used for light microscopic analysis and granule size distribution determination.

Fractionation of starch granules

Approximately 5 g of transgenic starch from clone *amf*SS#22 was fractionated by sieving (20 µm DIN-ISO 3310/1, Retsch, Haan, Germany), using a continuous flow of distilled water. Two fractions were obtained (with granules smaller and larger than 20 µm), which were air-dried at room temperature.

Trypsin treatment of starch granules

In order to test whether the various multiple SBD proteins are present inside starch granules or at the

granular surface, 20 mg of starch was treated with a non-limiting amount of trypsin (Sigma-Aldrich Chemie B.V.) as described by Ji et al. (2003). The result of trypsin digestion was evaluated by Western blot analysis. Digestion of bovine serum albumine with trypsin was performed to verify that the protease was active.

Results

Characterization of SBDn transformants

SBD2 was introduced into the KD background, yielding the KDSS#xx transformants, where xx represents the clone number. Untransformed control plants are referred to as KD-UT. Plant and tuber morphology, and tuber yield of all transgenic plants were comparable to that of control plants (data not shown).

The levels of SBD2 protein accumulation in transgenic granules of the KDSS series were investigated by Western dot blot analysis. The SBD2 accumulating lines were divided into six classes (ranging from 0+ to 5+; see Fig. 1a) based on the amount of SBD2 protein associated with the starch granules, similar to the class-definition for the *amf*SS series described previously (Ji et al. 2004). The SBD2 accumulation in the KDSS series is summarized in Fig. 1b. For comparison, single SBD accumulation in the KDS series (Ji et al. 2003) and SBD2 accumulation in the *amf*SS series (Ji et al. 2004) are also indicated in Fig. 1b. It can be seen that larger amounts of SBD2 than SBD can be accumulated in the WT background. This is consistent with our previous observations in the *amf* background (Ji et al. 2004). Further, it is clear that much higher levels of SBD2 can be accumulated in *amf* granules than in amylose-containing ones, which is also in accordance with earlier observations for single SBD (Ji et al. 2003).

SBD3, SBD4, and SBD5 were introduced into the KD background, yielding the KDS3#xx, KDS4#xx, and KDS5#xx transformants, respectively. Also for the plants of these series, plant and tuber morphology, and tuber yield were not consistently different from that of control plants. The granules of the KDS3, KDS4 and KDS5 series were subjected to Western dot blot analysis to determine the amount of SBD accumulated (Fig. 1b). We hereby assume that the appended SBDs act as individual epitopes for the antibody, i.e., a protein consisting of five appended SBDs binds five times more antibody than a protein consisting of one SBD. It can be seen that more SBD3 than SBD2 can be accumulated in the starch granules, consistent with our expectation that SBD3 is a higher-affinity starch-binding protein than SBD2. Many transformants with granules belonging to the 4+ to 6+ class were obtained with the KDS3 series, similar to the *amf*SS series. Our data do not indicate that SBD4 and SBD5 have a higher affinity for starch than SBD3, because only very few transformants of the KDS4 and KDS5 series had starch belonging to the higher SBD accumulation classes. SBD2, SBD3, SBD4, and SBD5 are correctly

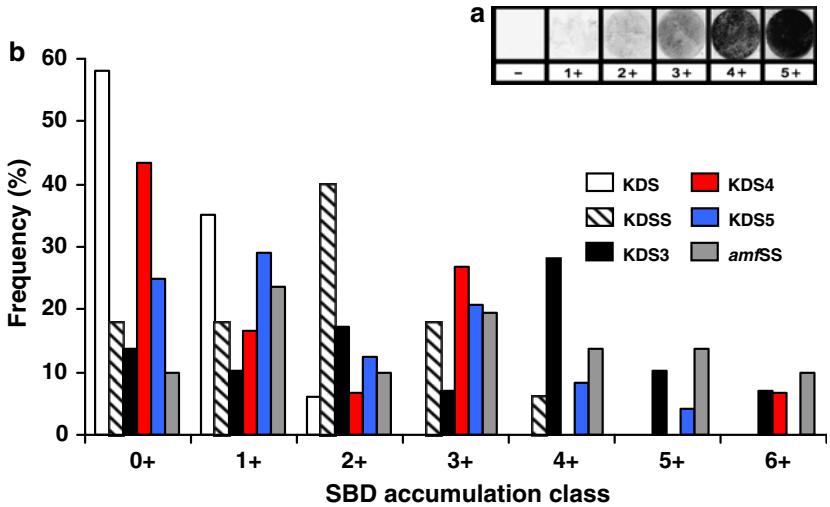

Fig. 1 Accumulation levels of SBD in potato starch granules isolated from the various series of transformants of the Kardal background (KDSS, KDS3, KDS4, and KDS5 series). **a** Classes of SBD accumulation in potato starch granules. This classification is based on the results of a Western dot blot analysis with various starch samples. The 6+ class represents the transgenic granules, which gave a similar signal in Western dot blot analysis as the 5+ class with half the amount of starch. **b** Distribution of the individual transformants over the seven classes of SBD accumulation in the Kardal background. SBD accumulation in the Kardal background (KDS series) and SBD2 accumulation in the *amf* background (*amf*SS series) are indicated for comparison

processed, as judged from the SDS polyacrylamide gel electrophoretic (SDS-PAGE) analysis combined with Western blot analysis using anti-SBD antibodies (Fig. 2a, left panel). Starch from the best KDSS transformant showed a band of approximately 26 kDa, whereas that of the best KDS3, KDS4, and KDS5 transformants had a single band of approximately 40, 55, and 75 kDa, respectively; this corresponded well to the predicted molecular masses of 25,371, 39,315, 53,157, and 66,999 Da for SBD2, SBD3, SBD4, and SBD5, respectively.

The location (inside the granule or at its surface) of SBD-containing proteins was determined by treating the starch of the best transformant of each series with trypsin, and comparing the amount of SBD associated with the granules, with and without treatment, by SDS-PAGE/Western blot analysis. No differences were observed between the treated and untreated samples (Fig. 3), demonstrating that the various SBD-containing proteins are mainly inside the starch granule, and that they do not (re)deposit on the granular surface during starch isolation. From previous research it is known that trypsin can degrade the SBD protein (Ji et al. 2003). The activity of the protease was verified by treatment of bovine serum albumine with trypsin, followed by SDS-PAGE analysis of the protein digest (data not shown).

The amount of SBDn protein was also determined (Western dot blot analysis) in the potato juice of one representative of each class from the various series. The results are summarized in Table 1. For comparison, the SBD2 concentration in the soluble fraction of representative *amf*SS potato tubers of each class (Ji et al. 2004) are also indicated. The amount of SBD2 found in class 1+ and 2+ KDSS tuber juice corresponded to the dot with an intensity of 1+ (see Fig. 1a), and that in class 3+ and 4+ KDSS tuber juice to 2+.

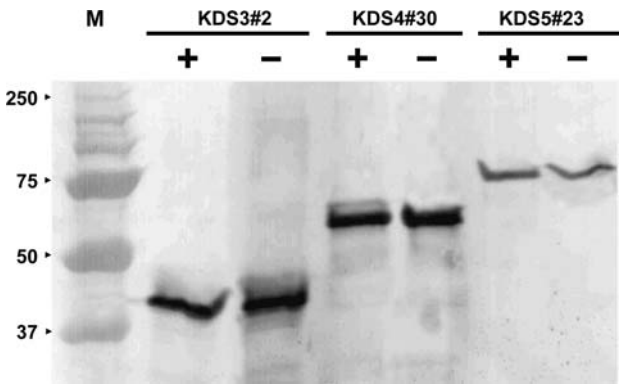

Fig. 3 Western blot analysis of the highest expresser of each multiple repeat SBD series, with and without trypsin treatment. Lanes marked + and − represent the granule-bound proteins in starch granules with and without trypsin treatment, respectively. Similar intensity of the bands in the + and − lanes indicates that the SBDn proteins are not accessible for the protease and are incorporated in the granule; a different intensity indicates that the SBDn protein is present at the surface of the granules. The molecular mass marker (*M*) is indicated as well, with the protein masses in kDa

Only trace amounts of SBD were present in the juices derived from the tubers of the various KDS3, KDS4, and KDS5 transformants. Typically, in the *amf*SS series, SBD2 can only be detected in the tuber juice derived of the 6+ class transformants, which suggests that the interaction of SBD2 with amylose-containing starch is of a different kind as with *amf* starch. Based on the Western dot blot results, one transgenic clone of a low (1+) and one of the highest accumulation class of the *amf*SS, KDSS, KDS3, KDS4 and KDS5 series were selected for Northern blot analysis, together with their respective controls (Fig. 4). The transcript levels of these transformants correlated well with the results obtained by the Western dot blot analysis, i.e., the transformants with starch granules of the 1+ class had low amounts of the transcript, whereas those with

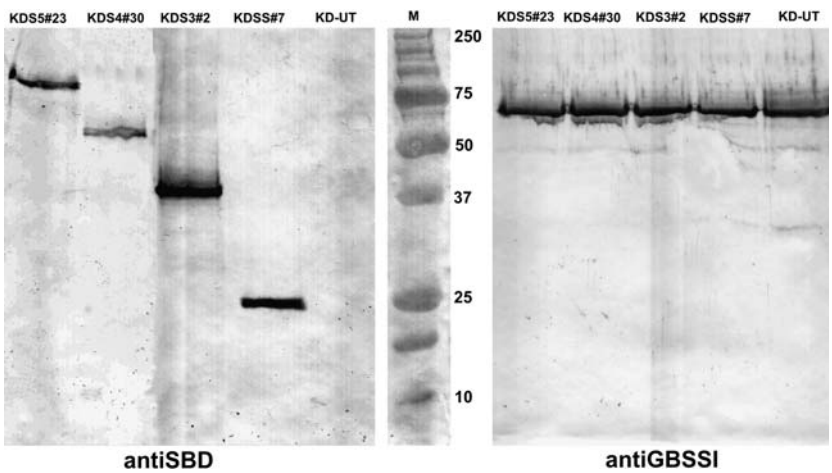

Fig. 2 Western blot analysis of the highest expresser of each multiple repeat SBD series. The untransformed control (KD-UT) is shown for comparison. After SDS polyacryl amide gel electrophoresis, the proteins were blotted onto a membrane, and probed with anti-SBD (*left panel*) and anti-GBSSI (*right panel*) antibodies. The molecular mass marker (*M*) is indicated as well, with the protein masses in kDa

Table 1 Accumulation levels of SBDn protein in juices of selected (transgenic) potato tubers of the KDSS, KDS3, KDS4, and KDS5 series

Amount of SBD in granules	Amount of SBD in potato juice				
	KDSS	KDS3	KDS4	KDS5	*amf*SS
0+	ND	Traces	ND	ND	ND
1+	1+	Traces	ND	ND	ND
2+	1+	Traces	ND	1+	ND
3+	2+	Traces	Traces	1+	ND
4+	2+	Traces	NA	1+	ND
5+	NA	Traces	NA	1+	ND
6+	NA	Traces	Traces	NA	2+

The amount of SBD2 in selected juices of the *amf*SS series are indicated for comparison. The number representation (1+, *etc.*) is according to the dot intensities in Fig. 1a

ND not detected, *NA* not applicable

starch granules of the higher classes had much higher amounts. SBD transcripts were absent in the untransformed controls.

Does expression of SBDn influence expression of key genes involved in starch biosynthesis?

In order to assess whether expression of multiple appended SBDs influenced the gene expression pattern of key genes in starch biosynthesis, quantitative real time RT-PCR was performed with the most severe transformants from each series. No significant differences in the expression level of AGPase SBEI, Susy, SSSIII, Stisa1, Stisa2, and Stisa3 were found in comparison to that of control plants (Fig. 5), demonstrating that the expression of the various SBD-containing constructs does not affect the expression of starch biosynthetic genes.

Amylose content of starch granules of SBDn transformants

The starch granules of each transformed clone of the various series of transformants were stained with a Lugol solution, and subsequently the granules were investigated for the presence of amylose by light microscopy. No decrease in the amount of amylose was apparent in the granules from any of the clones (data not shown). In order to detect smaller differences in amylose content, also a colorimetric amylose determination was performed with starch samples of each SBD accumulation class of the various series of transformants. In all samples, an amylose content (approximately 20%) similar to the untransformed control was found. These data demonstrate that neither the introduction of SBD2 nor that of multiple-repeated SBDs (SBD3, SBD4, SBD5) in an amylose-containing background could reduce the amylose content.

GBSSI content of starch granules of SBDn transformants

It has been shown previously that the GBSSI protein is present in surplus in potato starch granules, and that a reduction in the GBSSI content of the granules does not necessarily correlate with less amylose (Flipse et al. 1996). Therefore, we also determined the GBSSI content of the starch granules of the best KDSS, KDS3, KDS4, and KDS5 transformants by SDS polyacrylamide gel electrophoresis, followed by Western blotting using anti-GBSSI. The analysis was repeated three times. No consistent differences in the amount of GBSSI were found in comparison to starch from KD-UT, with any of the transgenic starch samples (Fig. 2, right panel). These results suggest that all the multiple-repeat SBDs are unable to displace GBSSI from the starch granule during the biosynthesis process, or that they bind at a different location within the starch granule.

Starch granule morphology

Starch granule morphology of each transformed clone from the KDSS, KDS3, KDS4, KDS5 and *amf*SS series were investigated by light microscopy. The selected micrographs of various KDSS and *amf*SS starch granules and their corresponding controls are shown in Fig. 6. It can be seen that KD-UT and KDSS#50 (1+) starch granules are phenotypically similar, except for the presence of apparent cracks in the granules. Further analysis of these granules by SEM showed that their surface was smooth (data not shown), indicating that the pronounced staining (cracks) does not represent a

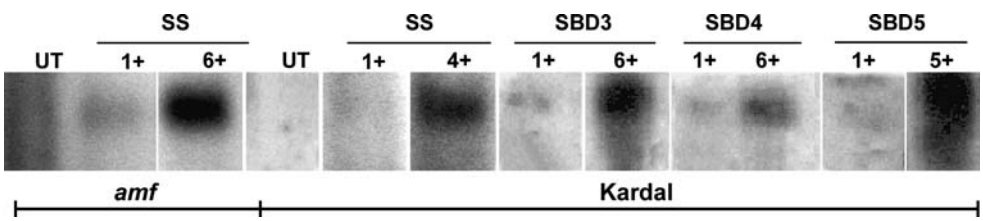

Fig. 4 Northern blot analysis of high and low expressers of different multiple SBDs, together with their respective controls. Each lane contained 40 µg of total RNA

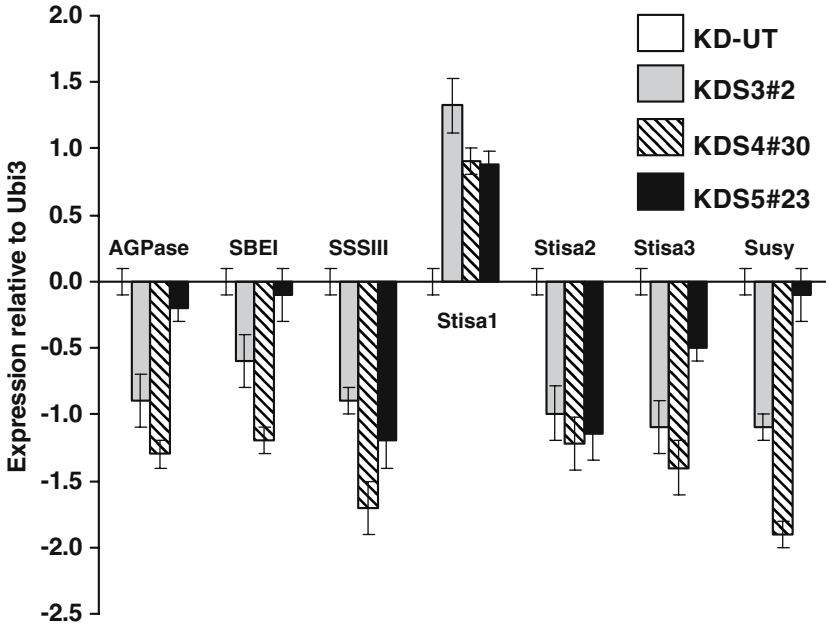

Fig. 5 Real-time quantitative RT-PCR analysis of RNA from the highest expresser of each multiple repeat SBD series and KD-UT. Primers specific for important genes in potato starch biosynthesis were used: ADP-glucose pyrophosphorylase (*AGPase*), starch branching enzyme I (*SBEI*), soluble starch synthase III (*SSSIII*), three isoforms of isoamylase (Stisa1, Stisa2, and Stisa3), and sucrose synthase (*Susy*). RNA levels for each gene were expressed relative to the amount of *Ubi3* RNA

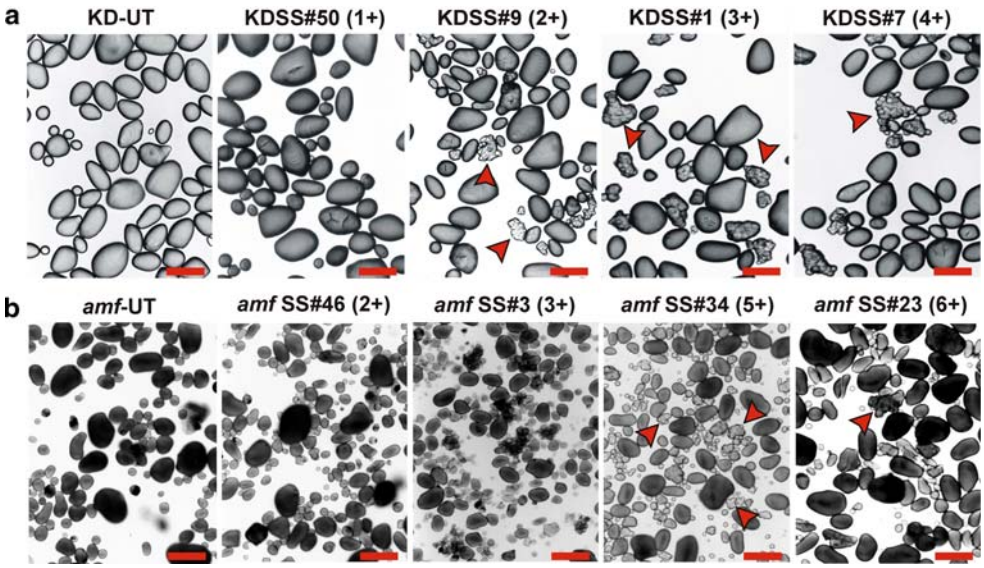

Fig. 6 Light micrographs showing the morphology of control and transgenic starch granules. The granules were stained with a 20× diluted Lugol solution. **a** Representative granule preparations of selected plants of KD-UT and the KDSS series. **b** Representative granule preparations of selected plants of *amf*-UT and the *amf*SS series. *Arrow heads* indicate amalgamated clusters. *Scale bar* represents 40 μm

groove in the surface, but rather a slightly altered internal organization. Such apparent cracks were also observed with single SBD, although they seem to be less pronounced. Higher SBD2 accumulation levels in the KDSS series showed altered granule morphology in both light and scanning electron micrographs. Granules were sometimes organized in amalgamated clusters. It seemed that this phenomenon was most pronounced in KDSS#1 (3+) and KDSS#7 (4+), although it could also be observed in KDSS#9 (2+). Starch from the various classes of KDS3, KDS4, and KDS5 transformants gave similar results, and there seems to be a tendency that, within one series of transformants, starches belonging to class 2+ and upwards show the amalgamated clusters at higher frequency than those of the lower accumulation classes (data not shown). The *amf*SS#3 starch contained loosely associated clusters. In *amf*SS#34 and *amf*SS#23 with higher levels of SBD2 than *amf*SS#3, these loosely associated clusters were not observed, but amalgamated clusters of very small granules were encountered. Thus, the amalgamated clusters are observed in both the Kardal and the *amf* backgrounds, but in Kardal they appear at lower levels of SBD2 accumulation.

Analysis of KDSS, KDS3, KDS4, KDS5 and *amf*SS granules by SEM revealed the clustered appearance of starch granules in more detail. Figure 7a shows a magnification of amalgamated clusters of very small granules in the Kardal background, whereas the loosely associated clusters of the *amf*SS#3 starch are shown in

Fig. 7b; the granules of the latter, but not of the former, could be cut loose by α-amylase treatment, indicating that the small granules were connected through α-glucans (data not shown). The micrographs of KDS3#2, KDS4#30, and KDS5#23 also showed the amalgamated clusters (Fig. 7d–f), similar to starches derived from the KDSS series (Fig. 7a, c). The size and frequency of appearance of the amalgamated clusters did not seem to be correlated to the number of appended SBDs.

Starch granules with SBD2 can assemble differently

In the starch granules from a number of transformants of the KDSS series, we observed the contour lines of amalgamated clusters of small granules inside larger starch granules (Fig. 8a, b). The normal, concentric pattern of growth rings was absent in these granules. Furthermore, it can be seen that normal-looking granules and granules with internalized amalgamated clusters can both occur in the starch of KDSS transformants. Similar observations were made for starches from the KDS3, KDS4, and KDS5 series. This phenomenon was not observed in the starch granules from any of the *amf*SS transformants. These data suggest that the irregular amalgamated clusters can grow out to mature granules.

Since the morphology of the granules appeared very different, a number of the starches were investigated by microscopy under polarized light. The untransformed controls, KD-UT and *amf*-UT, clearly showed the characteristic "Maltese cross" in the starch granules (Fig. 8d). The starches from the KDSS series (Fig. 8f), as well as those from the *amf*SS and other multiple SBD series (data not shown), showed an altered birefringence pattern. It appeared as if a large portion of the granules were built from many small ones, because often one granule contained many "Maltese crosses". This indicates that the radial molecular ordering within these granules is different from the starches that do not contain SBD2 (or multiple SBD).

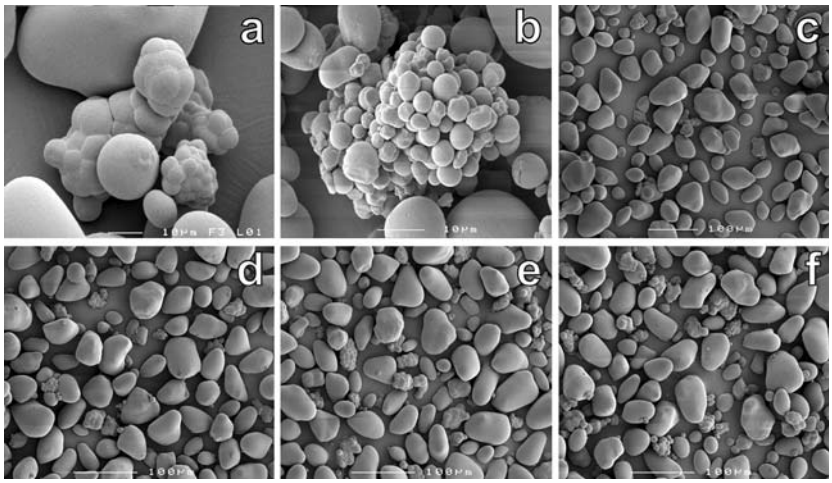

Fig. 7 SEM analysis of transgenic starch granules from the KDSS, KDS3, KDS4, KDS5, and *amf*SS series. **a** KDSS#1 (3+): close-up of amalgamated clusters. **b** *amf*SS#3 (3+): close-up loosely associated cluster. **c** KDSS#7 (4+). **d** KDS3#2 (6+). **e** KDS4#30 (6+). **f** KDS5#23 (4+). The granule size is indicated by the *scale bar*

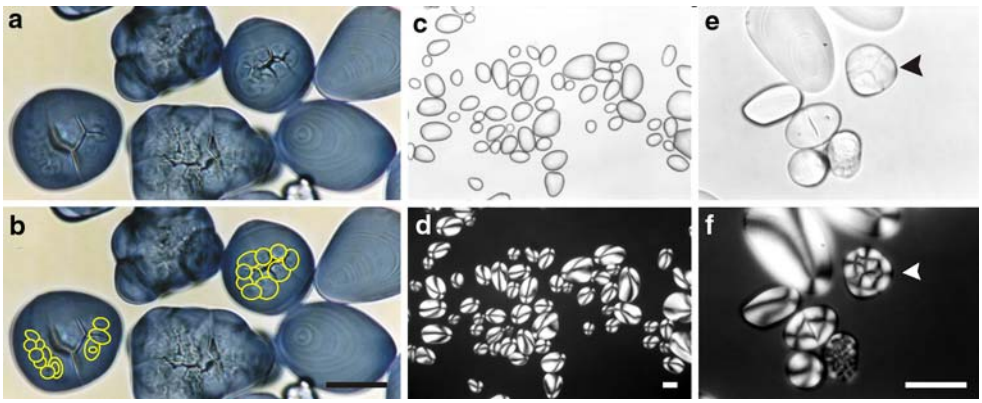

Fig. 8a-f Light micrograph of KDSS#2 (2+) starch granules stained with a 10× diluted Lugol solution. **a** Original image of the starch granules. **b** Same image, highlighting in yellow the contour lines of amalgamated clusters of small granules, which seem to be incorporated in larger starch granules. **c-f** Light micrographs of starch granules of KD-UT (**c, d**) and KDSS#9 (**e, f**) viewed under normal (**c, e**) and polarized light (**d, f**). *Arrow heads* indicate granules with multiple Maltese crosses. *Scale bar* represents 25 μm

Granule size distribution

The granule size distributions of all transgenic Kardal starch clones were determined. Additionally, the starches from transformants expressing SBD2 in the *amf* background were analyzed. For SBD2 transformants (both the Kardal and *amf* background), all granule size distributions recorded within one class of transformants were averaged, the result of which is summarized in Fig. 9a. The averaged granule size distributions of the starch of the various classes of the KDSS series were not deviated from the profile of the control, indicating that the granule size of the KDSS starches is not affected by SBD2 accumulation in the granules. This was not observed with the *amf*SS series; there, the granule size distribution became bimodal with increasing SBD2 accumulation. Furthermore, it seemed as if the smaller granules in the bimodal distribution become smaller with increasing SBD2 accumulation, and the larger ones larger. The granule size distributions of the KDS3, KDS4, and KDS5 transformants gave similar results as found with the KDSS series; the granule size distribution was unaltered, irrespective of the amount of SBDn accumulated.

Although the triplicate measurements with the Coulter Multisizer appeared to be very reproducible for each (transgenic) starch sample, we found a large variation in granule size distributions within one SBD2 accumulation class, particularly in the 3+ class of the *amf* background. An example of this is provided in Fig. 9b, which shows three different granule size distributions of starches belonging to the 3+ class: *amf*SS#3 has very small starch granules (mean granule size 7.8 μm), whereas *amf*SS#57 has relatively large ones (mean granule size 13.3 μm). *Amf*SS#25 had a bimodal distribution with peaks at 7.0 and 27.2 μm.

Fractionation of starch granules

In order to investigate the relationship between granule size and the level of SBD2 accumulation in the granule, the *amf*SS#22 starch (6+ class) with a bimodal granule size distribution was fractionated into granules larger and smaller than 20 μm. Microscopic examination revealed that the size of the starch granules in the two fractions was more uniform than in the starting material (data not shown), which was further substantiated by measuring the granule size distributions of the two starch fractions (Fig. 10a). Subsequently, the amount of SBD2 was determined in the two granule fractions by Western dot blot analysis. It appeared that the small granules contained more SBD2 protein than the larger ones (Fig. 10b).

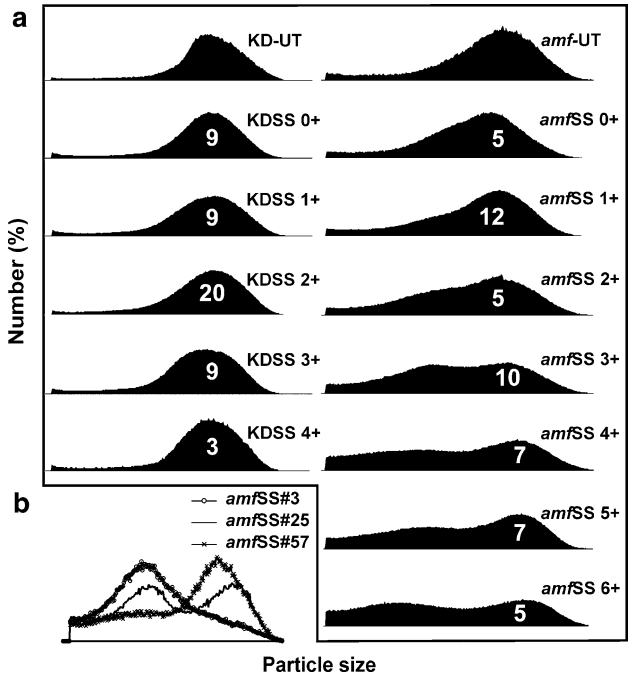

Fig. 9 Relationship between particle size distributions of the various starches and their SBD accumulation levels. **a** Averaged particle size distributions of the transgenic starches of the various SBD2 classes of the KDSS and *amf*SS series. Each starch sample was analyzed in triplicate, and the granule size distribution profiles of all starches belonging to the same class were averaged. The *number* inside the distribution indicates the number of transformants belonging to that class. **b** Averaged particle size distributions of *amf*SS#3, *amf*SS#25, and *amf*SS#57 transgenic starches from the 3+ class

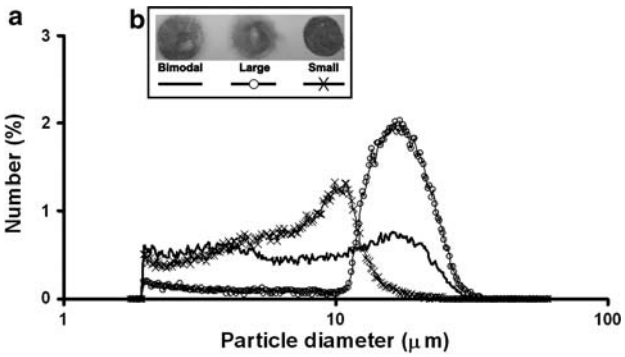

Fig. 10 Relationship between particle size distribution and SBD2 protein accumulation in *amf*SS#22 starch and its two constituent fractions. **a** Bimodal particle size distribution of the unfractionated *amf*SS#22 starch (*solid line*) and its two fractions after sieving: larger (*solid line with circles*) and smaller than 20 μm (*solid line with crosses*). **b** Amount of SBD2 in the unfractionated *amf*SS#22 starch (*bimodal*), and that in the large and small granule fraction

Starch content and physico-chemical properties of the starches

The impact of SBDn accumulation in granules on their physico-chemical properties and on the starch content of the tubers was investigated for the KDSS series. For this, one transgenic clone from each SBD accumulation-class of each series and their respective controls were selected. The starch content of the selected transformants and their controls were measured. Granule-melting behaviour (T_0 and ΔH) of the selected transgenic clones and their controls were investigated by differential scanning calorimetry (DSC). The results showed that there were no consistent differences in the various parameters between the transgenic starches and their controls (data not shown), similar to the results for the *amf*SS series reported before (Ji et al. 2004).

Schwall et al. (2000) inhibited the expression of both starch branching enzymes in potato tubers, and observed that the birefringence patterns of these transgenic starches were different from untransformed controls. Because there seems to be a relationship between birefringence and branching enzyme activity, the same transgenic starches as which were used for polarized light microscopy were investigated for differences in their chain-length distribution. With both high-pH anion-exchange chromatography (HPAEC; good separation of maltodextrins up to a degree of polymerization of approximately 45) and high-performance size-exclusion chromatograhy (HPSEC; a broader range separation than HPAEC, but with lower resolution), no differences were found between transgenic starches, and between transgenic starches and the respective untransformed controls (data not shown).

Since the granule packing appeared to be affected by the presence of SBD2, three *amf*SS and two KDSS starches were selected for X-ray diffraction analysis. The untransformed and transgenic starch granules all consisted of B-type crystallites, demonstrating that SBD2 expression did not alter the crystal type. Small, but consistent, differences in the crystallinity of the granules were found. The *amf*-UT starch had a crystallinity of 42%, that of *amf*SS#3 (3+) 45%, that of *amf*SS#22 (6+) 44% (the small and large granule fraction of *amf*SS#22 were also measured, and gave crystallinity values of 42 and 46%, respectively), and that of *amf*SS#23 (6+) 47%. The KD-UT starch had a crystallinity of 42%, that of KDSS#9 (2+) 39%, and that of KDSS#7 (4+) 42%. This suggests that there is no apparent correlation between the amount of SBD2 in the granule and crystallinity. Thus, the altered packing of the starch granule does not seem to lead to a different crystallinity of the granules.

Discussion

In this study, engineered high-affinity multiple-repeat SBDs were introduced into the amylose-containing potato genotype Kardal to investigate whether they could displace GBSSI from the starch granule during biosynthesis. Higher amounts of SBD2 than of SBD could be accumulated, which was similar to our previous observations in the *amf* background (Ji et al. 2004). SBD3 seemed to have a higher affinity for starch than SBD2 (Fig. 1), but the data on the affinity for starch of SBD4 and SBD5 are not conclusive. None of the multiple appended SBD proteins had the ability to reduce the GBSSI content of the starch granule, and therewith the amylose content. As it has been shown that the affinity for the target ligand of a protein increases with the number of carbohydrate-binding module repeats (Boraston et al. 2002; Ji et al. 2004), it was anticipated that particularly SBD4 and SBD5 would prevent GBSSI from binding the growing granule. As this does not occur, it seems most straightforward to assume that GBSSI and SBD bind different sites inside the starch granule. However, it cannot be excluded that they bind at similar sites. For this, it is important to consider the mechanism by which SBD binds α-glucans. This mechanism has been most extensively studied for the SBD of *Aspergillus niger* glucoamylase (Southall et al. 1999; Giardina et al. 2001; Paldi et al. 2003; Morris et al. 2005); the SBD of *Bacillus circulans* cyclodextrin glycosyltransferase, used in this study, is believed to display similar features (Kok-Jacon et al. 2003). SBD has two binding sites with distinct affinities for maltooligosaccharides. It is believed that the small and accessible site 1 is responsible for the initial recognition, whereas the longer site 2 is involved in tighter binding and undergoes conformational changes upon binding (Giardina et al. 2001). Paldi et al. (2003) observed that binding of SBD to starch granules is not instantaneous (unlike the binding of certain cellulose-binding domains), but requires approximately one hour, which seems to be consistent with the fact that site 2 needs to be moulded onto the α-glucan. After one hour, binding of SBD to starch was irreversible (see Fig. 11a). Furthermore, SBD with its two binding sites has been shown to induce conformational changes in linear α-glucan (Giardina et al. 2001), and it has been suggested that they can bind (and unwind) the non-reducing termini of two parallel side chains of amylopectin engaged in a double helix (Morris et al. 2005). When SBD and GBSSI are simultaneously present, as during starch biosynthesis, it might be that GBSSI displays an instantaneous, higher initial affinity for α-glucan than SBD, and that the conformational change of SBD's binding

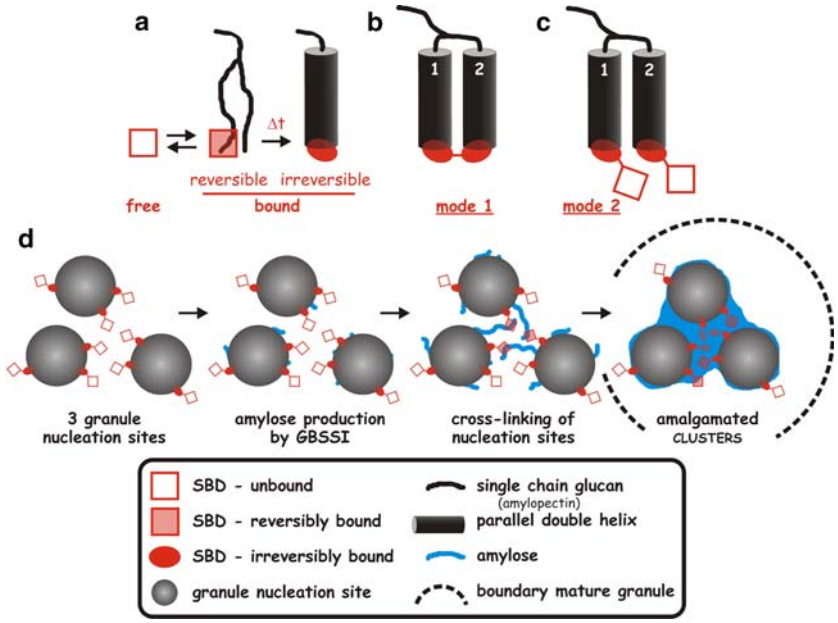

Fig. 11 Schematic representation of possible binding mechanisms and modes of SBD2. **a** SBD can bind the non-reducing termini of the double-helical side chains of amylopectin with high affinity, as suggested by Morris et al. (2005). Initially, binding site 1 of SBD is suggested to be involved in the initial, instantaneous recognition of α-glucan (reversible binding). Subsequently, SBD undergoes a conformational change to facilitate the stronger interaction of binding site 2 with the parallel, double helical amylopectin side chains (Giardina et al. 2001). This process requires time and is thought to be irreversible (Paldi et al. 2003). These double helices can be bound by SBD at high-affinity (irreversible). **b** At low SBD2 concentrations, both domains are expected to interact with the same granule surface (*mode 1*). **c** At higher SBD2 concentrations, the surface area may become limiting, and both domains can not be accommodated on the same surface anymore. Consequently, the SBD2 proteins may have one SBD attached to a double helix, whereas the other one is available for interaction with soluble glucans or amylose protruding from the granule surface (*mode 2*). **d** SBD2 binds in mode 2 to granule nucleation sites (note that only a few SBD2 proteins are shown). The exposed SBD of SBD2 is available for interaction with amylose-like molecules produced by GBSSI. If the exposed SBD of SBD2 binds amylose-like molecules from a different nucleation site, then the amalgamated clusters may be formed, which eventually develop into a starch granule

site 2 simply takes too much time for making SBD a true competitor of GBSSI. By increasing the number of SBDs in the fusion protein, the initial affinity for α-glucan might be enhanced; as it is possible that the appended SBDs interact with different α-glucan chains on the growing granule, this does not necessarily mean that SBDn has more competitive power than SBD alone, and therefore displacement of GBSSI is not self-evident. The above is consistent with our observations: (1) SBD and SBD2 can be accumulated in larger amounts in *amf* than in Kardal starch granules; and (2) more SBD2 was found in the tuber juices of all KDSS transformants than in those of the *amf*SS series, which hints at a more reversible binding in the Kardal background (in the *amf* background, SBD2 was only found in transformants with 6+ class granules, suggesting that the binding is of a more high-affinity type, and that the granule surface was only saturated in these high expressers).

Although SBD2 (Ji et al. 2004), and likely also SBD3, has more affinity for the starch granule than a single SBD, our data for SBD4 and SBD5 are not conclusive in this respect; the lower frequency of SBD4 and SBD5 transformants in the higher SBD accumulation classes compared to that of SBD3 transformants was unexpected (Fig. 1). Given the large amount of transcript found in the KDS5 (5+) transformant [Fig. 4; compare with SBD3 (6+)], it seems unlikely that an altered transcription of these multiple-repeat genes underlies this phenomenon. It might be that translation or import into the amyloplast becomes less efficient with proteins of more than three SBD repeats, but this was not further investigated, and needs to be substantiated. It can also not be excluded that the SBD antibody cannot bind all domains in proteins with more than 3 appended SBDs, leading to an underestimation of the amount of SBD-containing protein. However, in that case, we would have expected less high SBD accumulators (4+ to 6+) in the KDS5 series in comparison with the KDS4 series.

SBD2 seems to interfere with various aspects of the starch biosynthesis process, i.e., granule packing and granule morphology (Kardal and *amf*), and granule size (*amf*). For this, it is important to realize that SBD2

can bind to starch granules in two modes. In mode 1 (Fig. 11b), both SBDs of SBD2 are attached to the same granule surface. This mode presumably occurs at lower SBD2 concentration, when not all granule surface is covered with SBD. In mode 2 (Fig. 11c), one SBD binds the granule surface, whereas the other one is exposed to the granule surrounding. This mode might occur at higher SBD2 concentration, when the granule surface is saturated with SBD. We speculate that at low SBD2 concentration in the *amf* background mode 1 predominates, whereas at higher SBD2 levels in the *amf* background, and at any SBD2 concentration in the Kardal background, mode 2 becomes more important (see also Ji et al. 2004). The exposed SBD of SBD2 in mode 2 (or the "cross-linking" mode) might capture soluble glucans from the stroma or protruding amylose (Fig. 11d), and cross-link different granule nucleation sites, eventually leading to the clusters: the amalgamated ones (Kardal, *amf* high SBD2 expressers), and the loosely associated ones (*amf* intermediate expressers). The amalgamated clusters are observed in Kardal at lower levels of SBD2 accumulation than in the *amf* background. This might be due to the presence of amylose protruding from the granule surface, which may facilitate cross-linking of the small granules. The larger granules seem to have over-grown the clustered appearance, and develop into normal-looking ones (although multiple "Maltese crosses" occur within one granule; see Fig. 8f). It seems as if SBD2 is present in non-limiting amounts at the onset of starch biosynthesis, and becomes limiting at a certain time point in starch biosynthesis, after which the clustering stops, and the granules develop normally.

We have reported previously that SBD2 expression can reduce granule size in the *amf* background, depending on the amount of SBD2 accumulated (Ji et al. 2004). In the intermediate to high SBD2 accumulators (3+ to 6+ classes) of the *amf*SS series, bimodal granule size distributions were observed, a phenomenon, which is common for wheat starch (Peng et al. 2000). A thorough study in which granule size is monitored during tuber development might shed more light on this. Preliminary studies have indicated that small and large granules occur in one tuber cell, but also this needs further investigation. In the Kardal background, the granule size distributions are not affected by the presence of multiple appended SBDs, irrespective of the amount accumulated. This is consistent with SBDn binding mainly in mode 2 (see above) and the production of amylose close to the granule surface, the combination of which facilitates cross-linking of small granules. Typically, larger granules than those present in tubers of control plants are not formed. However, expression of SBD2 in the *Arabidopsis sex1* mutant leads to larger starch granules, and interestingly the starch granules from this mutant have a higher amylose content than those from wild type *Arabidopsis* (Howitt et al. 2006). Some caution is required with this extrapolation, as one compares transitory starch (*Arabidopsis*) to storage starch (potato), and a mutant in starch degradation (*Arabidopsis*) to a mutant in starch biosynthesis (potato).

At moderate to high SBDn accumulation in the Kardal background, it was observed that the assembly of oval-shaped granules was impaired (Fig. 7a, c–f). A kind of clustered appearance of starch granules was also observed by Howitt et al. (2006). Altered granule morphology has also been evidenced in other transgenic potato tubers, but in all these cases an enzyme activity involved in starch biosynthesis had been down-regulated (Edwards et al. 1999b; Lloyd et al. 1999a; Schwall et al. 2000; Fulton et al. 2003; Bustos et al. 2004). In these examples, the ratio of α-1,4 to α-1,4,6 linked glucose was altered in comparison to starch from untransformed potato plants, as evidenced from clear differences in chain-length distributions. In our study, the chain-length distribution of the various transgenic starches was unaltered, irrespective the amount of SBDn accumulated, and so were the expression levels of major starch biosynthetic genes. Therefore, it seems unlikely that the activity of starch synthase, branching enzyme and/or isoamylase is affected to any large extent. Our results and those from Howitt et al. (2006) suggest that differences in granule morphology can be mediated by protein binding only, a process by which the physical interactions between the constituent α-glucans can be modified; alterations in enzyme activities do not seem necessarily required. We believe that by using mutant (e.g., in the residues mediating binding of glucan) SBD2 (or SBDn), and fusing various partner proteins to SBD2, the physical interactions at play during starch biosynthesis can now be probed further.

References

Boraston AB, McLean BW, Chen G, Li A, Warren RAJ, Kilburn DG (2002) Co-operative binding of triplicate carbohydrate-binding modules from a thermophilic xylanase. Mol Microbiol 43:187–194

Bustos R, Fahy B, Hylton CM, Seale R, Nebane NM, Edwards A, Martin C, Smith A (2004) Starch granule initiation is controlled by a heteromultimeric isoamylase in potato tubers. Proc Natl Acad Sci USA 101:2215–2220

Edwards A, Borthakur A, Bornemann S, Venail J, Denyer K, Waite D, Fulton D, Smith A, Martin C (1999a) Specificity of starch synthase isoforms from potato. Eur J Biochem 266:724–736

Edwards A, Fulton DC, Hylton CM, Jobling SA, Gidley M, Rössner U, Martin C, Smith AM (1999b) A combined reduction in activity of starch synthases II and III of potato has novel effects on the starch of tubers. Plant J 17:251–261

Flipse E, Keetels CJAM, Jacobsen E, Visser RGF (1996) The dosage effect of the wildtype GBSS allele is linear for GBSS activity but not for amylose content: absence of amylose has a distinct influence on the physico-chemical properties of starch. Theor Appl Genet 92:121–127

Fulton DC, Edwards A, Pilling E, Robinson HL, Fahy B, Seale R, Kato L, Donald AM, Geigenberger P, Martin C, Smith AM (2003) Role of granule-bound starch synthase in determination of amylopectin structure and starch granule morphology in potato. J Biol Chem 277:10834–10841

Giardina T, Gunning AP, Juge N, Faulds CB, Furniss CSM, Svensson B, Morris VJ, Williamson G (2001) Both binding sites of the starch-binding domain of *Aspergillus niger* glucoamylase are essential for inducing a conformational change in amylose. J Mol Biol 313:1149–1159

Hovenkamp-Hermelink JHM, de Vries JN, Adamse P, Jacobsen E, Witholt B, Feenstra WJ (1988) Rapid estimation of the amylose/amylopectin ratio in small amounts of tuber and leaf tissue of potato. Potato Res 31:241–246

Howitt CA, Rahman S, Morell MK (2006) Expression of bacterial starch-binding domains in *Arabidopsis* increases starch granule size. Func Plant Biol 33:257–266

Ji Q, Vincken J-P, Suurs LCJM, Visser RGF (2003) Microbial starch-binding domain as a tool for targeting proteins to granules during starch biosynthesis. Plant Mol Biol 51:789–801

Ji Q, Oomen RJFJ, Vincken J-P, Bolam DN, Gilbert HJ, Suurs LCJM, Visser RGF (2004) Reduction of starch granule size by expression of an engineered tandem starch-binding domain in potato plants. Plant Biotechnol J 2:251–260

Jobling SA, Westcott RJ, Tayal A, Jeffcoat R, Schwall GP (2002) Production of a freeze-thaw-stable potato starch by antisense inhibition of three starch synthase genes. Nat Biotechnol 20:295–299

Kok-Jacon GA, Ji Q, Vincken J-P, Visser RGF (2003) Towards a more versatile α-glucan biosynthesis in plants. J Plant Physiol 160:765–777

Kok-Jacon GA, Vincken J-P, Suurs LCJM, Visser RGF (2005) Mutan produced in potato amyloplasts adheres to starch granules. Plant Biotechnol J 3:341–351

Kossmann J, Lloyd J (2000) Understanding and influencing starch biochemistry. Crit Rev Plant Sci 19:171–226

Kuipers AGJ, Jacobsen E, Visser RGF (1994) Formation and deposition of amylose in the potato tuber starch granule are affected by the reduction of granule-bound starch synthase gene expression. Plant Cell 6:43–52

Laemmli UK (1970) Cleavage of structural proteins during the assembly of the head of bacteriophage T4. Nature 227:680–685

Lloyd JR, Landschütze V, Kossmann J (1999a) Simultaneous antisense inhibition of two starch synthase isoforms in potato tubers leads to accumulation of grossly modified amylopectin. Biochem J 338:515–521

Lloyd JR, Springer F, Buleon A, Müller-Röber B, Willmitzer L, Kossmann J (1999b) The influence of alterations in ADP-glucose pyrophosphorylase activities on starch structure and composition in potato tubers. Planta 209:230–238

Morris VJ, Gunning AP, Faulds CB, Williamsson G, Svensson B (2005) AFM images of complexes between amylose and *Aspergillus niger* glucoamylase mutants, native and mutant starch binding domains: a model for the action of glucoamylase. Starch 57:1–7

Murashige T, Skoog F (1962) A revised medium for rapid growth and bioassay with tobacco tissue culture. Physiol Plant 15:473–497

Paldi T, Levy I, Shoseyov O (2003) Glucoamylase starch-binding domain of *Aspergillus niger* B1: molecular cloning and functional characterization. Biochem J 372:905–910

Peng M, Gao M, Båga M, Hucl P, Chibbar RN (2000) Starch branching enzymes preferentially associated with A-type starch granules in wheat endosperm. Plant Physiol 124:265–272

Schwall GP, Safford R, Westcott RJ, Jeffcoat R, Tayal A, Shi Y-C, Gidley MJ, Jobling SA (2000) Production of very-high-amylose potato starch by inhibition of SBE A and B. Nat Biotechnol 18:551–554

Southall SM, Simpson PJ, Gilbert HJ, Williamson G, Williamson MP (1999) The starch-binding domain from glucoamylase disrupts the structure of starch. FEBS Lett 447:58–60

Visser RGF (1991) Regeneration and transformation of potato by *Agrobacterium tumefaciens*. Plant Tiss Cult Man B5:1–9

Visser RGF, Suurs LCJM, Bruinenberg PM, Bleeker I, Jacobsen E (1997a) Comparison between amylose-free and amylose containing potato starches. Starch 49:438–443

Visser RGF, Suurs LCJM, Steeneken PAM, Jacobsen E (1997b) Some physicochemical properties of amylose-free potato starch. Starch 49:443–448

Vos-Scheperkeuter GH, de Boer W, Visser RGF, Feenstra WJ, Witholt B (1986) Identification of granule-bound starch synthase in potato tubers. Plant Physiol 82:411–416

Wakelin JH, Virgin HS, Crystal E (1959) Development and comparison of two X-ray methods for determining the crystallinity of cotton cellulose. J Appl Phys 30:1654–1662